

Nonequilibrium Green's function calculation for four-level scheme terahertz quantum cascade lasers

H. Yasuda,^{1,2,a)} T. Kubis,³ P. Vogl,³ N. Sekine,² I. Hosako,² and K. Hirakawa¹

¹*Institute of Industrial Science and Institute for Nano Quantum Information Electronics, University of Tokyo, 4-6-1 Komaba, Meguro-ku, Tokyo 153-8505, Japan*

²*National Institute of Information and Communications Technology, 4-2-1, Nukui-Kitamachi, Koganei, Tokyo 184-8795, Japan*

³*Walter Schottky Institute, Technische Universität München, Am Coulombwall 3, 85748 Garching, Germany*

(Received 18 February 2009; accepted 23 March 2009; published online 15 April 2009)

We have calculated the performance of a recently proposed four-level scheme terahertz quantum cascade laser (4L terahertz-QCL) with the nonequilibrium Green's function method. The calculation result for 40 K showed that the 4L QCL has a larger terahertz gain than the conventional resonant phonon QCL. This is because a large number of electrons accumulate in the upper lasing level and contribute to lasing in the new scheme. When the temperature is increased, the advantage of gain decreases due to thermally activated phonon scattering. © 2009 American Institute of Physics. [DOI: 10.1063/1.3119312]

Remarkable progress on terahertz quantum cascade lasers (terahertz-QCLs) has been made since their first demonstration in 2002.^{1,2} Low-frequency operation at 1.2 THz,³ high continuous wave output power of 138 mW,⁴ and high operation temperature at 178 K (Ref. 5) have been achieved for terahertz-QCLs. However, operation of terahertz-QCLs at room temperature has not yet been realized. Operation temperatures of resonant phonon QCLs,^{4,5} which are thought to be appropriate for high-temperature operation, tend to be limited by hf/k_B (k_B is the Boltzmann constant). Recently, some attempts were made to introduce a four-level (4L) scheme to the QCLs.^{6–8} These ideas intend to improve electron injection to the upper lasing level. Although the 4L scheme QCLs appear to be similar to the double resonant phonon QCL,⁹ where electrons in the lower lasing level are scattered twice by longitudinal optical (LO) phonons, the “indirect-pump” 4L QCLs proposed by Yamanishi *et al.*^{7,8} differs from the double resonant phonon scheme in that electrons are scattered directly to the upper lasing level by the second LO phonons. Operation of the indirect-pump 4L QCL at 8 μm with a low threshold current density of 2.7 kA/cm² and a high output power of 362 mW at room temperature was reported.⁷ The characteristic temperature T_0 at 303 K of this laser is the highest among reported QCLs, which implies excellent temperature stability of the threshold current. The indirect-pump 4L QCL might have potential for room-temperature operation in the terahertz frequency range.

In this work, we have calculated the performance of the indirect-pump 4L terahertz-QCL by using the nonequilibrium Green's function theory (NEGF) and considered its advantage and feasibility for high-temperature operation. The NEGF is a first-principle calculation method first developed in the 1960s by Keldysh¹⁰ and Kadanoff and Baym¹¹ and applied to the analysis of QCLs by several groups.^{12–14} The details of our NEGF program are largely based on the study of Lake *et al.*¹⁵ In our calculation, a real-space eigenbasis¹⁶ was used and the QCL is treated as an open quantum device using lead self-energies.¹⁴ The electrons are described within

a one-band model with an effective mass. The acoustic phonon, optical phonon, charged impurity, and interface roughness scatterings are taken into account as self-energies evaluated within the self-consistent Born approximation. Electron-electron interaction was treated in the Hartree approximation. Dyson's equation, Keldysh relation, and Poisson's equation were solved self-consistently until the retarded Green's function $G^R(z, z', \mathbf{k}_\parallel, E)$ and the correlation function $G^<(z, z', \mathbf{k}_\parallel, E)$ converged. The position coordinates z and z' were taken in the direction of the crystal growth, \mathbf{k}_\parallel the in-plane wave vector, and E the total energy.

Figures 1(a) and 1(b) illustrate the spectral functions $A(z, E) = i[G^R(z, z, \mathbf{0}, E) - G^{R\dagger}(z, z, \mathbf{0}, E)]$ and the conduction band diagrams for one period of the conventional resonant phonon and the indirect-pump 4L QCLs, respectively.^{8,17} The maxima of the spectral function represent resonant states. We define the injector, active, and ejector regions as shown in Figs. 1(a) and 1(b) for convenience. One period of the resonant phonon QCL sequence is **3.0/9.0/5.5/8.1/2.7/6.3/4.1/15.3** nm. The bold and regular numbers represent Al_{0.15}Ga_{0.85}As and GaAs layers, respectively. The underlined quantum well is n -doped with $n = 1.2 \times 10^{16}$ cm⁻³. To reduce memory consumption, the structure was drawn in the 0.9 nm pitch mesh in our NEGF calculation. Therefore, the barriers not matching with the mesh were adjusted with the effective barrier height. The applied electric field was set to 9.3 kV/cm. On the other hand, one period of the indirect-pump 4L QCL sequence was taken as **1.8/9.9/2.7/7.2/2.7/14.4/0.9/9.9/3.6/17.1** nm. The bold and regular numbers represent Al_{0.23}Ga_{0.77}As and GaAs layers, respectively. The underlined 9.9-nm-thick quantum well is n -doped at the level of 1.2×10^{16} cm⁻³. The applied electric field was 16.0 kV/cm. The left and right sides of both QCLs are connected to the electrodes. We developed a “quasiperiodic” contact model to express the periodic nature of the QCL.¹⁴ The width of the rightmost barrier around $z=60$ nm in Fig. 1(a) was set to be the same as that of the leftmost barrier. The chemical potentials in the contacts were determined by (i) the global charge neutrality of the device and (ii) the applied voltage drop between the contacts. It has been demonstrated that this way

^{a)}Electronic mail: yasuda@nict.go.jp.

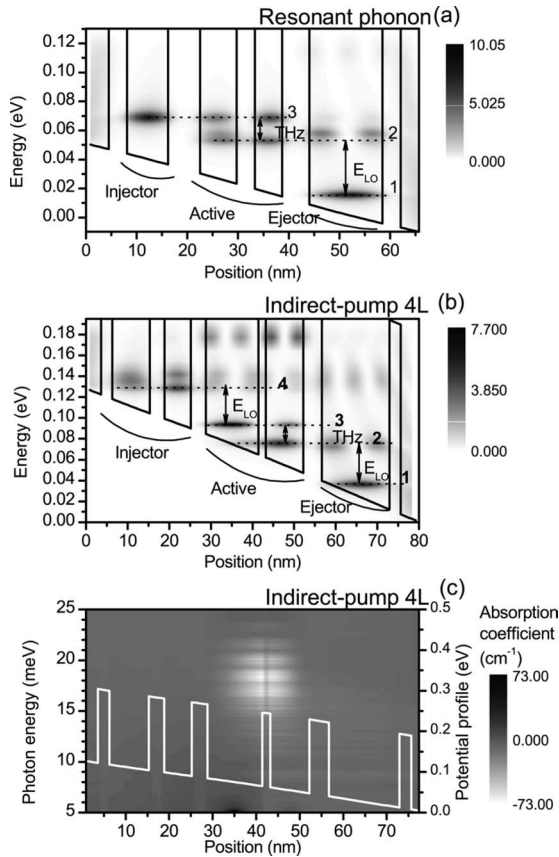


FIG. 1. [(a) and (b)] Conduction band schematics of the resonant phonon QCL and the indirect-pump 4L QCL, respectively, calculated using the NEGF program. Contour plots represent the spectral function $A(z, E)$. (c) Absorption coefficient $\alpha(z, \omega)$ of the indirect-pump 4L QCL.

of treating the contacts has negligible influences on the calculated results.¹⁴ This allows us to limit our calculations on one period of the QCL. For both QCLs, the lower lasing levels (labeled with 2) are depopulated by the resonant emission of LO phonons. The LO phonon energy E_{LO} in GaAs is 36 meV. In the conventional design given in Fig. 1(a), the upper lasing level (labeled with 3) is aligned with the left-most state and is resonantly filled. In contrast, in the indirect-pump 4L QCL of Fig. 1(b), electrons are injected to level 4 and scattered from level 4 to the upper lasing level (labeled with 3) by emission of LO phonons. Here, no resonant tunneling contributes to the filling of the upper lasing level. On this point, the new QCL differs from conventional resonant phonon QCLs.

To obtain optical gain, the optical field is included as perturbation to the Hamiltonian. Then, the changes in the Green's functions and self-energies caused by the perturbation, the change in the current density, and the complex susceptibility are calculated.¹² Since the Green's functions are expressed by the real-space eigenbasis, the z -dependence of the absorption coefficient can be obtained. Figure 1(c) shows the calculated absorption coefficient $\alpha(z, \omega)$ of the indirect-pump 4L QCL as a function of position and photon energy at 40 K. The local optical gain is observed mainly in the two wells defined as the active region. The maximum local optical gain in Fig. 1(c) reaches 73 cm^{-1} at 4.4 THz, while that of the resonant phonon QCL remains 10 cm^{-1} at 3.0 THz. The total gain over one period of the indirect-pump 4L QCL is 14 cm^{-1} , which is significantly larger than that of the resonant phonon QCL of 4 cm^{-1} , although the number of doped

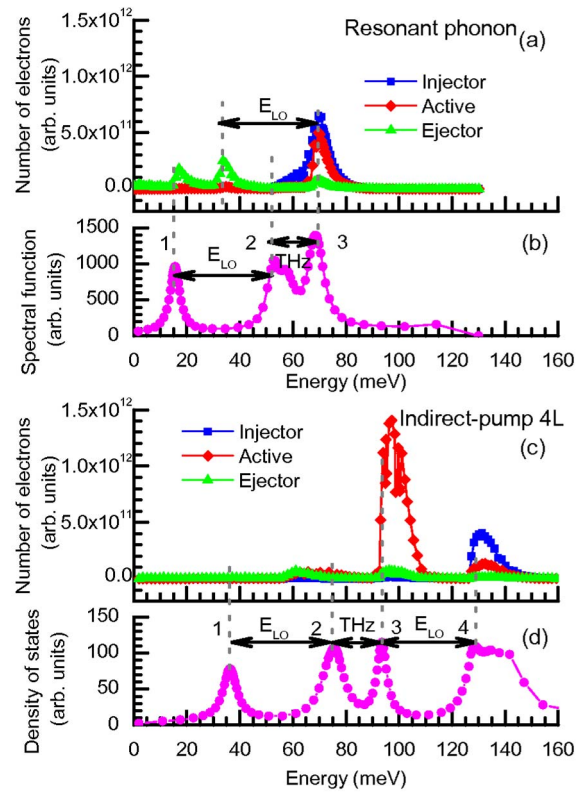


FIG. 2. (Color online) (a) Energy-resolved electron distributions in the injector, active, and ejector regions of the resonant phonon QCL at 40 K. (b) Spectral functions, that is, density of states with $k_{\parallel}=0$ of the QCL at 40 K. [(c) and (d)] The same as (a) and (b) for the indirect-pump 4L QCL.

impurities in the former QCL is slightly lower than that in the latter. This can be explained by the number of electrons that contribute to the laser oscillation. Figures 2(a) and 2(b) show the energy-resolved electron distributions $\int \rho(z, E) dz = -2 \int dz \text{Im} \int dk_{\parallel} G^{<}(z, z, k_{\parallel}, E) / (2\pi)^3$ in the injectors, active regions, ejectors, as well as the spectral functions $\int A(z, E) dz$ averaged over one entire QCL period for the resonant phonon QCL at 40 K. Figures 2(c) and 2(d) show those for the indirect-pump 4L QCL. The distribution peak in the ejector of the conventional QCL around 35 meV in Fig. 2(a) shows electrons scattered by LO phonons from the upper lasing level (labeled as 3) in the active region. As further illustrated in Fig. 2(a), less than one half of the electrons are situated in the upper lasing level in the active region of the resonant phonon QCL. In contrast, the electrons in level 4 of the indirect-pump 4L QCL are relaxed quickly to the upper lasing level (level 3) by the LO phonon scattering. Therefore, as can be seen in Fig. 2(c), almost all the electrons are populated in the upper lasing level in the active region of the indirect-pump 4L QCL, which leads to larger optical gain.

We also performed similar calculations for the two QCL structures at 200 K. The temperature changes the electron distribution in the electrodes and the temperature of the phonon bath. It also changes the Debye screening length with which the interaction with LO phonons and charged impurities is screened. The maximum local gain of the conventional resonant phonon QCL was 3 cm^{-1} . That of the indirect-pump 4L QCL decreased dramatically to 5 cm^{-1} , compared to 73 cm^{-1} obtained at 40 K. The reduction in gain can be explained using electron distributions. Figures 3(a)–3(d) show the energy-resolved electron distributions and the spec-

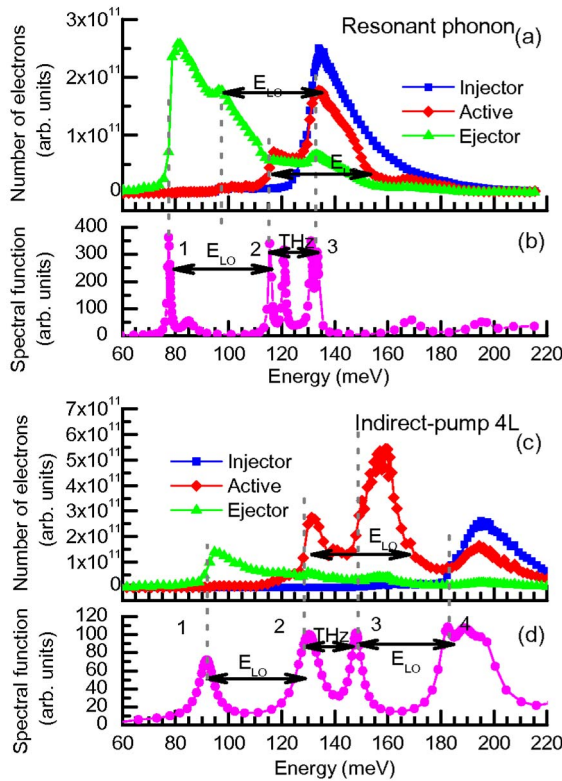


FIG. 3. (Color online) The same as Fig. 2 at 200 K. [(a) and (b)] The resonant phonon QCL. [(c) and (d)] The indirect-pump 4L QCL.

trum functions averaged over one QCL period of the conventional resonant phonon and the indirect-pump 4L QCLs at 200 K. Two degradation mechanisms of population inversions of terahertz-QCLs at high temperatures have been proposed.² One is thermal backfilling, by which electrons in the lasing levels are backfilled from the lower levels by thermal excitation. The other is thermally activated phonon scattering, where electrons in the upper lasing level acquire sufficient in-plane kinetic energy to emit an LO phonon and relax to the lower lasing level in a nonradiative manner. For the resonant phonon QCL, thermal backfilling is clearly observed in Fig. 3(a) as the electron distribution curve of the ejector region extending from the lowest level (level 1) to the lower lasing level (level 2). Thermally activated phonon scattering is also revealed in Fig. 3(a). The electron distribution curve of the active region has a dip around 155 meV. The energy difference between the dip and the lower lasing level 2 is about E_{LO} . This indicates that the electrons in the upper lasing level acquire thermal energy and those excited to the states around 155 meV are scattered by the LO phonon to the lower lasing level 2.

In contrast, the thermal backfilling effect in the indirect-pump 4L QCL has little influence on the degradation of the population inversion as shown in the electron distribution in the ejector region in Fig. 3(c). This is because few electrons populate in the lowest level (level 1) in the indirect-pump 4L QCL. The main cause of the population inversion degradation for the indirect-pump 4L QCL is thermally activated

phonon scattering. Many electrons populate in the upper lasing level, which is a feature of the indirect-pump 4L QCL, as shown in the electron distribution in the active region in Fig. 3(c). However, the number of electrons scattered by thermally activated phonon scattering is almost proportional to that in the upper lasing level. Therefore, the advantage of the indirect-pump 4L QCL deteriorates at high temperatures. One candidate to reduce the influence of thermally activated phonon scattering is the application of a high magnetic field to quench the lateral motion of electrons or the use of a material with a large LO phonon energy. Indirect-pump or resonant phonon QCLs using a GaN-based material system with GaN LO phonon energy of about 90 meV would be promising for high-temperature operation of terahertz-QCLs.

In summary, we simulated the performance of the indirect-pump 4L terahertz-QCL with the NEGF method. The simulation result for 40 K showed that the indirect-pump 4L QCL has a larger terahertz gain than conventional resonant phonon QCLs. The main reason for this is that a larger number of electrons contribute to lasing in the new scheme. However, the advantage of gain deteriorates at 200 K due to thermally activated phonon scattering.

We thank T. Kamiya, T. Ihara, Y. Sakasegawa, and S. Birner for fruitful discussions. This work is partly supported by the Grant-in-Aid from the Japan Society for the Promotion of Science (Grant No. 18201027), the Specially Coordinated Fund (NanoQuine) from MEXT, and the Österreichische Fonds zur Förderung der Wissenschaft (SFB IRON). The international collaboration program was partly supported by the Global COE program “Secure-life Electronics,” University of Tokyo.

¹R. Köhler, A. Tredicucci, F. Beltram, H. E. Beere, E. H. Linfield, A. G. Davies, D. A. Ritchie, R. C. Iotti, and F. Rossi, *Nature (London)* **417**, 156 (2002).

²B. S. Williams, *Nat. Photonics* **1**, 517 (2007).

³C. Walthers, M. Fischer, G. Scalari, R. Terazzi, N. Hoyler, and J. Faist, *Appl. Phys. Lett.* **91**, 131122 (2007).

⁴B. S. Williams, S. Kumar, Q. Hu, and J. L. Reno, *Electron. Lett.* **42**, 89 (2006).

⁵M. A. Belkin, J. A. Fan, S. Hormoz, F. Capasso, S. P. Khanna, M. Lachab, A. G. Davies, and E. H. Linfield, *Opt. Express* **16**, 3242 (2008).

⁶N. Sekine and K. Hirawaka, Japan Patent Application No. P2006-181502 (pending).

⁷M. Yamanishi, K. Fujita, T. Edamura, and H. Kan, *Opt. Express* **16**, 20748 (2008).

⁸M. Yamanishi, T. Edamura, N. Akikusa, and K. Fujita, Japan Patent Application No. P2006-236491 (pending).

⁹B. S. Williams, S. Kumar, Q. Qin, Q. Hu, and J. L. Reno, *Appl. Phys. Lett.* **88**, 261101 (2006).

¹⁰L. P. Keldysh, *Sov. Phys. JETP* **20**, 1018 (1965).

¹¹L. P. Kadanoff and G. Baym, *Quantum Statistical Mechanics* (Benjamin, New York, 1962).

¹²S.-C. Lee and A. Wacker, *Phys. Rev. B* **66**, 245314 (2002).

¹³R. Nelander and A. Wacker, *Appl. Phys. Lett.* **92**, 081102 (2008).

¹⁴T. Kubis, C. Yeh, and P. Vogl, *J. Comput. Electron.* **7**, 432 (2008).

¹⁵R. Lake, G. Klimeck, R. Bowen, and D. Jovanovic, *J. Appl. Phys.* **81**, 7845 (1997).

¹⁶S. Datta, *Superlattices Microstruct.* **28**, 253 (2000).

¹⁷A. Benz, G. Fasching, A. M. Andrews, M. Martl, K. Unterrainer, T. Roch, W. Schrenk, S. Golka, and G. Strasser, *Appl. Phys. Lett.* **90**, 101107 (2007).